PCCP

Physical Chemistry Chemical Physics

Accepted Manuscript

Volume 19
Number 1
7 January 2017
Pages 1-896

PCCP

Physical Chemistry Chemical Physics
rsc.li/pccp

ISSN 1463-9076

PAPER
H.-P. Loock et al.
Determination of the thermal, oxidative and photochemical degradation rates of scintillator liquid by fluorescence EEM spectroscopy

ROYAL SOCIETY OF CHEMISTRY

ROYAL SOCIETY OF CHEMISTRY

rsc.li/pccp

Formation of stable biradical triplet state cation versus closed shell singlet state cation by oxidation of adducts of 3,6-dimethoxycarbazole and polychlorotriphenylmethyl radicals.

Paola Ballesteros,[†,#] Alba Cuadrado,[⊥] Alejandra Gilabert,[†] Lluís Fajarí,[†] Ignasi Sirés,[‡] Enric Brillas,[‡] Maria Pilar Almajano,[#] Dolores Velasco,[⊥] Josep M. Anglada,[†*] Luis Juliá[†*]

[†]*Departament de Química Biològica i Modelització Molecular, Institut de Química Avançada de Catalunya (CSIC), Jordi Girona 18-26, 08034 Barcelona, Spain.*

[#]*Chemical Engineering Department, Universitat Politècnica de Catalunya, Av. Diagonal 647, 08028 Barcelona, Spain.*

[⊥]*Departament de Química Orgànica Institut de Nanociència i Nanotecnologia (IN²UB), Universitat de Barcelona, Martí Franquès 1-11, 08028 Barcelona, Spain.*

[‡]*Laboratori d'Electroquímica dels Materials i del Medi Ambient, Departament de Química Física, Facultat de Química, Universitat de Barcelona, Martí Franquès 1-11, 08028 Barcelona, Spain.*

E-mail: *ljbmoh@cid.csic.es, anglada@iqac.csic.es*

Abstract

We report an experimental and theoretical study of two stable radical adducts of the triphenylmethyl series, **1** and **2**, whose composition and molecular structure are distinguished by the content and position of chlorine atoms in phenyls. The electrochemical study through cyclic voltammetry of these open layer species

shows the existence of two reversible processes, related to a reduction and an oxidation, to stable charged species. The chemical oxidation of both radical adducts gives rise to stable cations, whose fundamental state has a biradical triplet electronic structure or a closed shell singlet character, depending on the electronic conjugation between the donor and acceptor electron moieties. The presence of chlorines adjacent to the nitrogen in **1** breaks the conjugation between both halves, facilitating the formation of a triplet electronic state of the cation, while the absence of the chlorines in these positions in **2** facilitates partial conjugation and stabilizes the closed shell singlet electronic state of the cation.

Introduction

Carbazole derivatives are a kind of organic compounds extensively investigated due to their applications in electronic devices in different technological fields.[1, 2] They have distinguished mainly as hole semiconductors due to the ease with which they lose an electron.[3] The electrochemical oxidation of carbazole derivatives is mainly characterized by the initial loose of an electron from the non-bonding pair on the nitrogen, giving rise to a radical cation. These cationic species are, in general, unstable and suffer dimerization, which can be prevented introducing substituents in the most active positions.[4, 5] As an example, polymers bearing pendent 3,6-dimethoxycarbazole units show reversible electrochemical oxidation.[6] In addition, carbazole has been part of organic materials with bipolar semi-conductivity as electron-donor group in donor-acceptor systems,[7-9] which are characterized by low ionization potentials and high electronic affinities that make them very favorable as optoelectronic devices.

In the last times, we have been involved in the study of the electronic properties of stable free radical adducts of the TTM [tris(2,4,6-trichlorophenyl)methyl radical][10] and DTM [tris(2,3,5,6-tetrachlorophenyl)methyl radical][10] series, using both radical species as electron-acceptor parts in binary systems, preparing radical adducts with bipolar semiconductivity incorporating carbazole derivatives to both organic free radicals.[11-20] These new radical adducts are characterized by their thermal and chemical stability and are prepared and isolated as pure solids, stable in solution. In turn, they present a) absorption bands in the visible part of the electronic spectrum, as charge transfer bands from the donor to the acceptor part of the molecule, b) electrochemical amphoteric behavior with two redox centers in the molecule that easily undergo oxidation and reduction, respectively, to stable charged species and c) magnetic properties due to the radical character of the molecule.

Very recently, Li and co-workers have produced organic light-emitting diodes (OLEDs) built from adducts between TTM and carbazole derivatives whose high efficiency is due, in great part, to the formation of a biradical in the oxidation step ("hole injection") of the whole process.[21] In connection to this, and taking advantage of the electrochemical stability of the oxidized species of these radical adducts, we now report the chemical oxidation of a new radical adduct of the DTM series, [4-(3,6-dimethoxy-9-carbazolyl)-2,3,5,6-tetrachlorophenyl]-bis(2,3,5,6-tetrachlorophenyl)methyl radical adduct (**1**) (Scheme 1), with a strong electron donating carbazole derivative as substituent, the 3,6-dimethoxycarbazole, and whose oxidation leads to the formation of a stable biradical cation. Their electronic structure and those of the oxidized species have been compared with the corresponding ones of the known radical adduct **2**[13]

(Scheme 1), which differs from **1** exclusively in the number and position of chlorine atoms of the triphenylmethyl moiety. In order to help to rationalize our results we have also carried out theoretical calculations on both **1** and **2** radicals and the corresponding cations in their triplet and closed shell singlet electronic states.
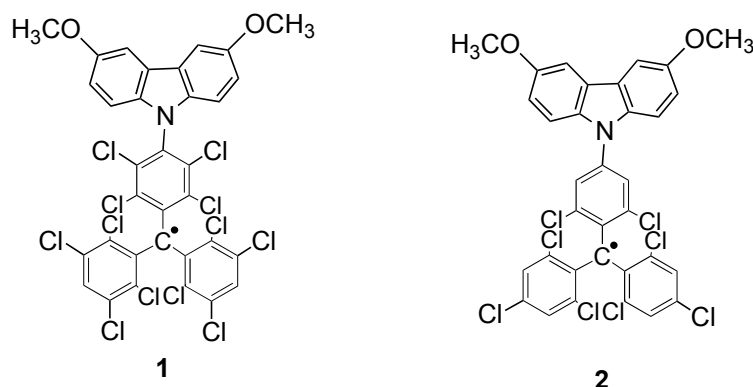

Scheme 1 Chemical structure of radical adducts 1 and 2

Results and Discussion.

The details of the synthesis and spectroscopic characterization of the compounds analyzed in this work are discussed in the Supplementary Information. The UV-vis-near infrared spectra of **1** in solvents with different polarity are displayed in Table S1 and Figure S1. Visible and near-infrared spectroscopy and paramagnetic electronic resonance (epr) have been used to characterize and differentiate the electronic structure of the oxidized species of both open-shell compounds. The theoretical work carried out in this investigation include geometry optimization and characterization calculations using the B3LYP[22] density functional approach, calculations on the electronic spectra in the framework of the Time-Dependent density functional theory[23] with the B3LYP

functional, and single point energy calculations at DLPNO-CCSD(T) level of theory.[24] Full details of the theoretical methods employed are also discussed in the Supplementary Information.

In Figure 1 we have drawn the optimized structures of radical adducts **1** and **2**, computed at B3LYP/6-31+G(2df) level of theory. The structure of **1** is very similar to that of [(4-N-carbazolyl)-2-3-5-6-tetrachlorophenyl]bis(2,3,5,6-tetrachlorophenyl)methyl radical reported recently,[11] as both compounds only differ in the methoxy-substituents in the N-carbazolyl moiety. The 2,3,5,6-tetrachlorophenyl bridge is almost perpendicular to the carbazolyl group, with a computed value of 93.4°, whereas the relative orientation of the three 2,3,5,6-tetrachlorophenyls are twisted by 49.6°, 49.7°, and 49.2°, so that the repulsion between the chlorine atoms is minimized. As pointed out in reference 10 this structure prevents the π delocalization between the carbazolyl moiety and the phenyl ring and the unpaired electron is mainly localized over the triarylsubstituted carbon atom which has a computed spin density of 0.73. On the other side, the lack of the two chlorine substituents in 3 and 5 in the dichlorophenyl bridge of **2** allows for a more flexible structure and the angle between the N-carbazolyl moiety and the substituted phenyl bridge is computed to be 65.8°, which allows an easier π delocalization between rings. In **2**, the radical is still localized over the triarylsubstituted carbon with a computed spin density of 0.67.

1 •   **2** •
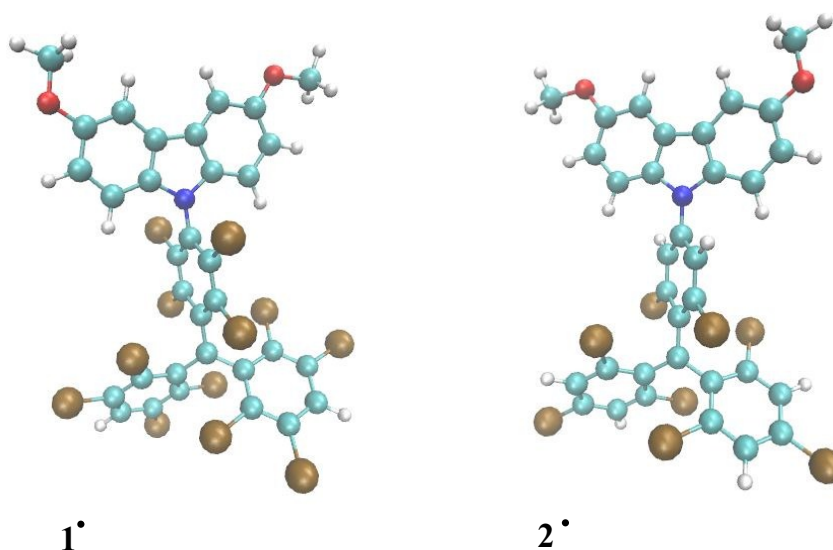
Fig. 1 UB3LYP/6-31+G(2df) optimized structures of radical adducts **1** and **2**. The dihedral angle between the phenyl bridge and the carbazolyl group in **1** is 93.4º and in **2** is 65.8º.

The main electronic features of **1** and **2** are displayed in Figure 2, where we have collected the corresponding frontier orbitals. This figure shows important differences between both radical adducts. In **1**, the two highly occupied molecular orbitals HOMO and HOMO-1 have computed orbital energies close to -5.40 and -5.95 eV and their electronic density is localized over the N-carbazolyl moiety exclusively, whereas the electronic density of the SOMO (singly occupied molecular orbital) is mainly localized over the triarylsubstituted carbon atom, as pointed out above, and it has an orbital energy of -6.33 eV, that is, about 0.9 and 0.4 eV smaller than those of HOMO and HOMO-1, respectively. Figure 2 also shows that for **2**, the topology and electronic features of the HOMO, HOMO-1 and SOMO orbitals are quite the same as those in **1**. However the SOMO orbital energy in **2** is destabilized by 0.55 eV relative to **1**, so that its orbital energy is closer to that of the β part of HOMO.
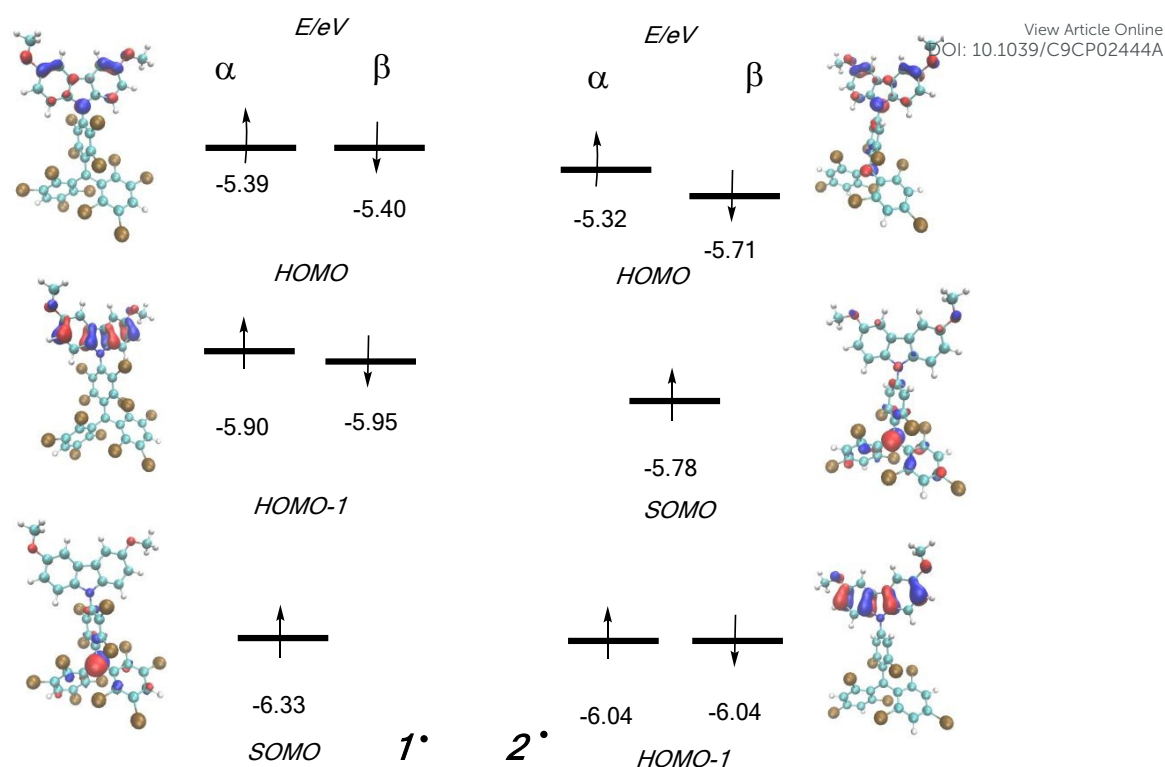
Fig. 2 Frontier orbitals of radicals **1** and **2** calculated at B3LYP/6-31+G(2df) level of theory. The arrows indicate the spin of the unpaired electron in each orbital.

These results suggest a different behavior regarding the oxidation of both radical adducts and, according to this picture, one would expect that oxidation of **1** would mainly imply ionization of one electron from the HOMO orbital leading to the formation of a biradical species (singlet or triplet electronic state) in the ground electronic state of the corresponding cation, whereas for **2**, this picture does not clearly allows to distinguish if the oxidation would imply ionization from the HOMO orbital (leading to the formation of a biradical structure) or ionization from the SOMO orbital (producing a closed shell cation). The different stability regarding the orbital energies in **1** and **2** may be attributed to the different rigidity of both structures, where a more flexible structure of **2** allows and easier π delocalization,

resulting in a smaller electron density of the unpaired electron over the triarylsubstituted carbon atom (see above).

The electrochemical behavior of radical adduct **1** has been studied through cyclic voltammetry. **1** exhibits two quasi-reversible one-electron processes (Figure 3), reduction by addition of one electron and oxidation by removal of one electron, to yield two stable charged species, anion and cation, respectively. Table 1 shows the redox potentials and the differences between the anodic and cathodic peaks of each process together with values from **2** for comparison.[13]
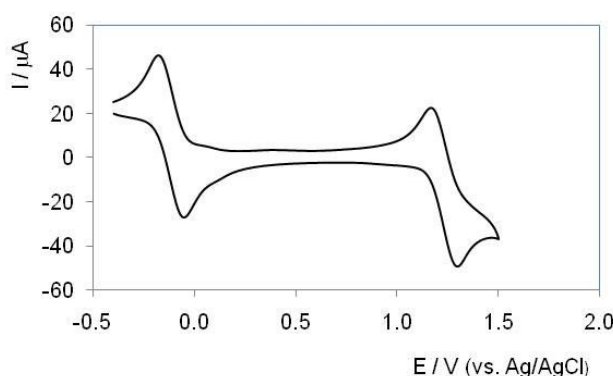
Fig. 3 Cyclic voltammogram for the reduction and the oxidation of radical adduct **1** (1 mM) in CH_2Cl_2 solution with 0.10 M TBAP on Pt at room temperature.

Table 1 Electrochemical properties of radical adducts **1** and **2** in CH_2Cl_2 solution with 0.10 M TBAP on Pt at room temperature.

| Compound	E^o_{red} (V)[a] $(E_p^a - E_p^c \text{ (mV)})$[b]	E^o_{oxi} (V)[c] $(E_p^a - E_p^c \text{ (mV)})$[b]	EA[d] (eV)	IP[e] (eV)	E_{gap}[f] (eV)
1	-0.12 (123)	1.23 (128)	4.34	5.57	1.23
2[g]	-0.54 (100)	0.86 (120)	4.26	5.66	1.40

[a] Standard potential vs. Ag/AgCl for the reduction pair. [b] Difference between anodic and cathodic peak potentials at a scan rate of 100 mV s^{-1}. [c] Standard potential vs. Ag/AgCl for the oxidation pair. [d] Electron affinity determined as EA = E^{red}_{onset} +4.4. [e] Ionization potential

determined as IP = E^{oxi}_{onset} +4.4. [f] Electrochemical gap calculated as the difference between IP and EA values. [g] Standard potential values for the reduction and oxidation pairs of **2** from reference [13].

An analysis of the results in Table 1 indicates that the standard potentials for the reduction and oxidation of both radical adducts **1** and **2** are influenced by the electron-acceptor moiety of the molecule, TTM or DTM. Both processes are reversible in **1** and **2**, confirming the stability of the reduced and oxidized species. While the chemical reduction of **1** (Figure S2 and Scheme S1) does not deserve special mention, we have focused our attention on the oxidation of **1** compared with the oxidation of **2** reported in the literature.[17]

For this, we have recorded the UV spectra during the oxidation process, where the bands of the radical adducts **1** and **2** disappear whereas the bands of the corresponding cations appear as the oxidation takes place. Figure 4a,b shows the evolution of the electronic spectra of radical adduct **1** in CH_2Cl_2 solution with an excess of $SbCl_5$. The emerging weak bands in the near-infrared spectrum at $\lambda = 767$ and $\lambda = 858$ nm are associated to typical bands of the carbazole radical cation of the molecule, which are shifted at longer wavelengths regarding the bands of the radical cation of 9-ethyl-3,6-dimethoxycarbazole ($\lambda = 682$ and 758 nm).[25] In the near ultraviolet region of the spectrum, the band at $\lambda = 378$ nm, attributed exclusively to the radical moiety ($\lambda = 373$ nm in DTM), remains practically constant in the oxidized species, while a new and weak band emerges at $\lambda = 499$ nm.
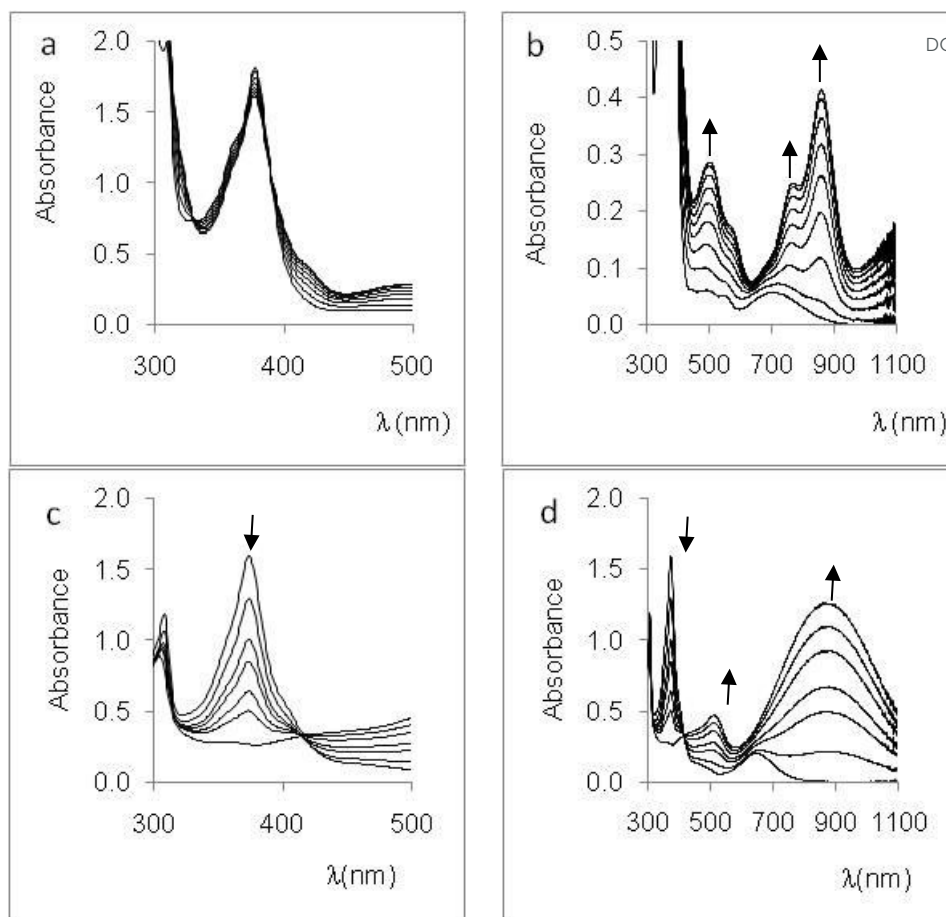
Fig. 4 a), b) Graphs at different wavelength intervals showing the evolution of the spectra of radical adduct **1** (6.6·10^{-5} M) with SbCl$_5$ (8.9·10^{-4} M) in CH$_2$Cl$_2$ solution in 2 h time. Bands at λ = 499, 768 and 858 nm increase, while band at λ = 378 nm remains practically constant. c), d) Graphs at different wavelength intervals showing the evolution of the spectra of radical adduct **2** (8.1·10^{-5} M) with increasing amounts of Cu(ClO$_4$)$_2$ in CH$_2$Cl$_2$, from reference [17]. Band at λ = 374 nm decreases, while bands at λ = 512 and 875 nm increase.

These results can be rationalized by calculating the spectra of the doublet electronic state (**^{2}1)** of radical adduct **1**, and the triplet and closed shell singlet electronic states of its cation **1$^+$**. The corresponding results are collected in Figure 5 (in the 300 – 1000 nm of wavelength range), and in Tables S2-S4 of the Supplementary Information. It is worth mentioning here that in the cation triplet state (**^{3}1$^+$**) the two unpaired electrons are localized one of them over the

triarylsubstituted carbon atom (which is the SOMO orbital in ^{2}1), and the other one over the nitrogen atom of the carbazole moiety, that is, it correlates with the radical ^{2}1 by ionization (oxidation) of and electron in the HOMO orbital, whereas the cation closed shell singlet state (^{1}1$^+$) correlates with the radical ^{2}1 by ionization (oxidation) of the unpaired electron in the SOMO orbital (see also Figure 2).
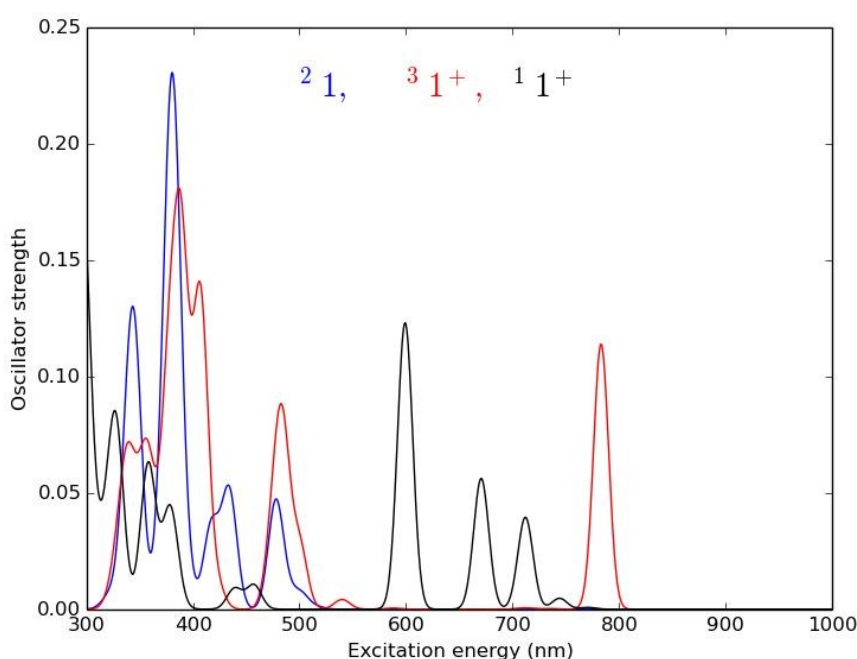
Fig. 5 Calculated electronic spectra, in the 300 – 1000 nm range, of radical ^{2}1 (in blue) and the triplet (^{3}1$^+$ in red) and closed shell singlet electronic states (^{1}1$^+$ in black) of the corresponding cation. A Gaussian function with an arbitrary sigma value of 100 has been used to draw the calculated spectra.

At first glance, Figure 5 shows that there is an overlap of the bands of the radical ^{2}1 with the bands of cation in its triplet electronic state (^{3}1$^+$) in the region between 300 – 500 nm. In both cases, these bands correspond to excitations of the unpaired electron from the triarylsubstituted carbon atom to anti-bonding orbitals of phenyl substituents, between 340 - 400 nm, and transitions from the π system

in the phenyl substituents to the single occupied orbital of the triarylsubstituted carbon atom, close to λ = 500 nm. Figure 5 also shows a band close to λ = 800 nm that is a fingerprint of the cation triplet state that corresponds to a transition from the π system of the carbazole moiety to the single occupied orbital over the nitrogen atom. On the other hand, Figure 5 also shows three bands, one around λ = 600 nm and two between 670 - 712 nm that constitute a signature of the closed shell singlet electronic state of the cation ($^1\mathbf{1^+}$), and correspond to excitation from the π system of the phenyl substituents and carbazole moiety to the empty (virtual) orbital of the triarylsubstituted carbon atom (see also Table S4). Looking at the above mentioned results of the spectra recorded along the oxidation process and displayed in Figure 4, the emerging bands at λ = 499 and close to λ = 800 nm can be associated to the formation of the triplet electronic state of the cation, and the strong band close to λ = 400 nm corresponds to both, the radical and the cation triplet state, but there are no bands between 600 - 700 nm, which lead us to conclude that the oxidation of **1** involves abstraction of one electron from the HOMO orbital, producing the cation in its triplet (biradical) electronic state, as suggested by the analysis of the orbital energies discussed above. Further evidence of these findings are given in Figure S3, which shows the evolution of the electronic spectra of the parent diamagnetic compound of **1**, **1H**, in CH_2Cl_2 solution in the presence of an excess of $SbCl_5$, for comparative reasons. The evolution of the spectra of **1H** with time in the interval 500 - 1000 nm is practically equal to the evolution of the spectra of **1**, with the emerging bands (λ = 505, 766 and 862 nm). Therefore, the oxidation in both species takes place in the carbazole, retaining the radical character of the triphenylmethyl carbon in **1**. These results on **1H** are also supported by theoretical calculations

as reported in Figure S4 and discussed in the Supplementary Information. Thus, the oxidation in **1** starts with the loss of one electron of the non-bonding pair on the nitrogen, giving a cation-diradical species $^3\mathbf{1}^+$ (Scheme 2).
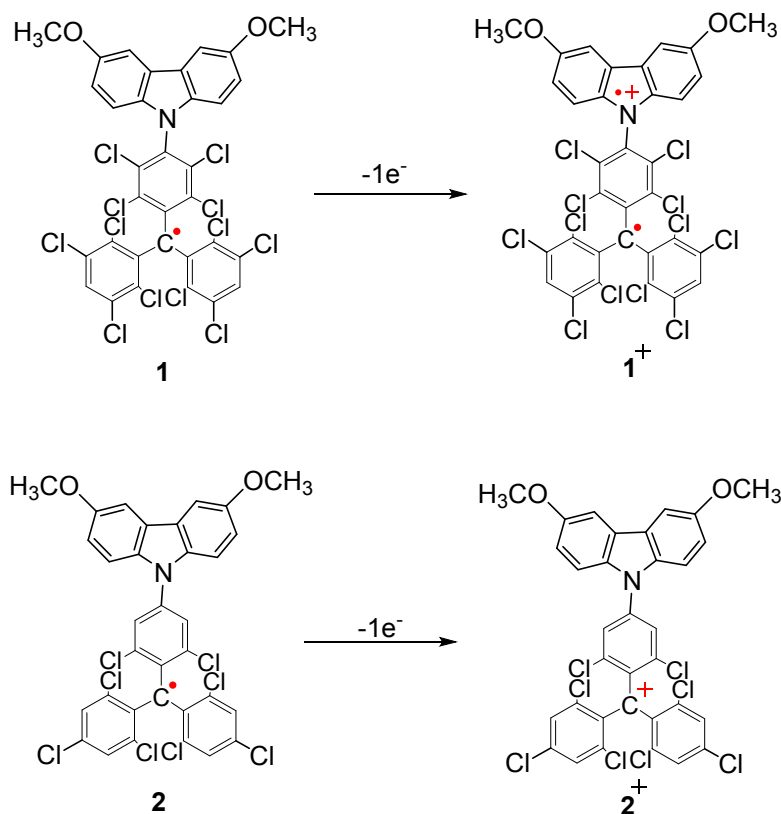

Scheme 2 Structures of the oxidized species from **1** and **2**

A very different behavior results when radical adduct **2** is oxidized, now with $Cu(ClO_4)_2$ as oxidant. "The absorption band characteristic of the radical character (λ = 374 nm) decreased with a concurrent increase of the absorption of two new bands at λ = 512 and 875 nm, the second being stronger and broader than the first one."[17] It seems as if the oxidation in **2** takes place in the trivalent carbon to give a carbocation **2**$^+$ (Scheme 2). These findings are also supported by the

results of the theoretical calculations. As for **1**, we have calculated the spectra of the radical **2** (^{2}**2** electronic state) and its corresponding cation **2**$^+$ in the triplet (^{3}**2**$^+$) and closed shell singlet (^{1}**2**$^+$) electronic states. The corresponding results are displayed in Figure 6 and in Tables S5-S7 of the Supplementary Information. Figure 6 shows a quasi-overlap of the bands of the radical ^{2}**2** and the cation ^{3}**2**$^+$ in the interval 370-410 nm, that correspond to excitations of the unpaired electron in the triarylsubstituted carbon atom to anti-bonding orbitals in the phenyl substituents. As stated above, these bands decrease and eventually disappear during the course of oxidation. The main signatures of the closed shell singlet electronic state of the cation (^{1}**2**$^+$) are computed to be at λ = 566 nm ($\pi_{diphenyl} \rightarrow$ $lp^*_{C\text{-}trialryl}$) and with very high intensity between 870 – 900 nm, ($lp_N \rightarrow lp^*_{C\text{-}trialryl}$; $\pi_{carb} \rightarrow lp^*_{C\text{-}trialryl}$) These bands appear along the oxidation process (see Figures 4c and 4d), being the second one a broad and strong band at λ = 875 nm. Thus, our results lead us to conclude that oxidation of radical ^{2}**2** involves ionization of the unpaired electron from the SOMO orbital, in contrast with the oxidation of **1** discussed above.

Regarding the single electronic states of cations **1** and **2**, (^{1}**1**$^+$, and ^{1}**2**$^+$), it should be pointed out here that we have only considered species having a closed shell structure, although excited electronic states having the same spin structure than the triplet states, namely with two open shells, should also exist. Such kind of singlet electronic states cannot be studied with mono-referential methods but they should lie higher in energy than the corresponding triplet electronic states[26] and, consequently, above the singlet closed shell electronic state in the case of **2**.
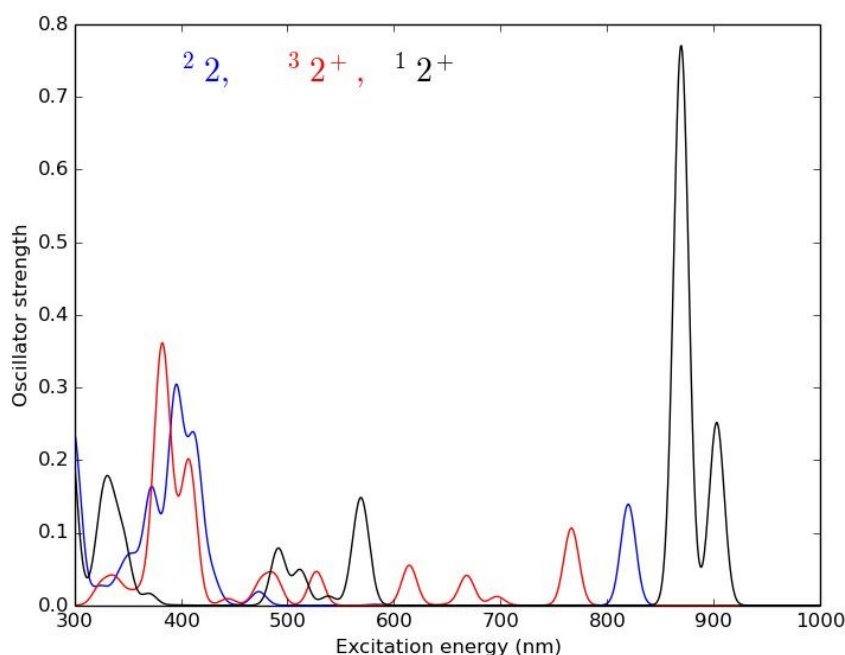
Fig. 6 Calculated electronic spectra, in the 300 – 1000 nm range, of radical **^{2}2** (in blue) and the triplet (**^{3}2$^+$** in red) and closed shell singlet electronic states (**^{1}2$^+$** in black) of their corresponding cations. A Gaussian function with an arbitrary sigma value of 100 has been used to draw the calculated spectra.

The presence of the cation in its triplet electronic state as the oxidized species of **1**, is also confirmed by electron paramagnetic resonance (epr). Figure 7 shows the epr spectrum of **1** with an excess of $SbCl_5$ in CH_2Cl_2. The spectrum at room temperature (Figure 7a) shows a single and wide band (ΔH_{pp} = 13.74 G) at g = 2.00332. The spectrum in glassy CH_2Cl_2 at 113 K (Figure 7b) presents the typical bands of a triplet state with the zero-field splitting energy parameters D = 122.24 G (0.0114 cm^{-1}) and E = 7.71 G (0.00072 cm^{-1}) and the anisotropic g-values, g_x = 2.00412, g_y = 2.00394 and g_z = 2.00535. The position of the three pairs of bands corresponds to a species with proximal to axial symmetry, although the E-parameter is not zero. The value of D-parameter indicates a relatively strong

dipolar spin-spin interaction and, therefore, a substantial singlet-triplet energy band. The bandwidths required for a very tight spectrum simulation of the experimental one ($\Delta H_{pp}(x)$ = 8.0 G, $\Delta H_{pp}(y)$ = 15.0 G, $\Delta H_{pp}(z)$ = 20.0 G) suggests the existence of undefined anisotropic couplings of the electron, mainly with the nitrogen nucleus. The central band in the spectrum is identified as a residual initial doublet species. As the parameter D is proportional to $1/R^3$, being R the average distance between the unpaired electrons, according to equation $2D = 3g^2\beta^2$ $(1/r^3)$,[27] the value for the diradical cation is R = 6.12 Å (calculated 5.745 Å). The isotropic and weak band centered at g = 4.00712 (ΔH_{pp} = 9.86 G) confirms the existence of the triplet state. The sequence of spectra of the oxidation of a more diluted solution of **1** ($6.6 \cdot 10^{-5}$ M) over time (every 5 min) is shown in Figure S5, and has the appearance of a wide band resulting from the electron-electron interaction.
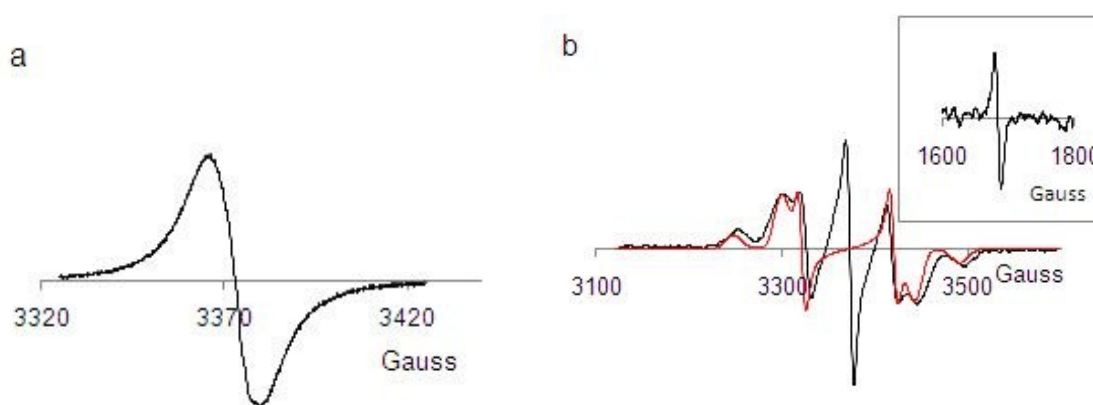
Fig. 7 X-band EPR spectra of the oxidation of radical adduct **1** (4.26×10^{-4} M) with an excess of $SbCl_5$ (12.5×10^{-3} M) in CH_2Cl_2. a) A single and broad (ΔH_{pp} = 13.74 G) band at room temperature and b) the fine structure of the $\Delta M_s = \pm 1$, at 113 K; zero-field splitting energy parameters D = 122.24 G (0.0114 cm^{-1}) and E = 7.71 G (0.00072 cm^{-1}) (insert the forbidden $\Delta M_s = \pm 2$ transition).

However, the sequence of epr spectra observed as the oxidation of **2** proceeds, leads to a continuous decrease in the intensity of the band until its complete disappearance (Figure S6). Thus, the initial doublet species is converted into a singlet species at room temperature, as indicated in Scheme 2, being completely transparent in the epr. The structural difference between molecules of **1** and **2**, responsible for this different behavior, lies in the presence of the two vicinal chlorine atoms to the carbazole substituent in **1** that are absent in **2**. These atoms are responsible for the strong distortion to the planarity between carbazole group and the phenyl bridge in **1**, giving rise to a total loss of conjugation between both moieties.

Finally, in order to further support the conclusions raised along this work we have also calculated the ionization energies of the radical adducts **1** and **2** leading to the formation of the corresponding triplet and closed shell singlet electronic states, respectively. The results, collected in Table 2 indicate that the triplet electronic state of the cation **1⁺** lies lower in energy than the cation in its closed shell singlet state by 0.32 eV whereas for **2**, **¹2⁺** lies lower than **³2⁺** by 0.28 eV. These results support the findings that oxidation of **1** produces the cation in its triplet electronic state whereas oxidation of **2** produces the cation in its closed shell singlet electronic state.

Table 2 Calculated oxidation energies (in eV) for radicals ²1 and ²2 leading to the formation of the corresponding singlet and triplet cations ¹1⁺, ³1⁺, ¹2⁺ and ³2⁺.[1]

Compound	Δ(E+ZPE)	Compound	Δ(E+ZPE)
²1·	0.00	**²2·**	0.00

$^3\mathbf{1}^+$	6.91	$^3\mathbf{2}^+$	6.80
$^1\mathbf{1}^+$	7.23	$^1\mathbf{2}^+$	6.52

(1) Computed at DLPNO-CCSD(T)/cc-pVTZ//B3LYP/6-31+G(2df) level of theory.

Conclusions

The reported results show different behaviour in the oxidation of two radical adducts of the TTM and DTM series. Ultraviolet, visible and near-infrared spectroscopy, and epr measurements together with theoretical calculations have shown that the oxidation of [4-(3,6-dimethoxy-9-carbazolyl)-2,3,5,6-tetrachlorophenyl]-bis(2,3,5,6-tetrachlorophenyl)methyl radical adduct (**1**) involves ionization of one electron of the lone pair over the nitrogen atom of the carbazole moiety rather than ionization of the unpaired electron of the radical, resulting in a biradical triplet electronic state in contrast with [4-(3,6-dimethoxy-9-carbazolyl)-2,6-dichlorophenyl]-bis(2,4,6-trichlorophenyl)methyl radical adduct (**2**), whose oxidation involves ionization of the unpaired electron of the radical producing a closed shell singlet electronic state. Both adducts differ exclusively in the number and position of chlorine atoms of the triphenylmethyl moieties so that in **1**, the conjugation between the donor and electron acceptor moieties is prevented favouring thus the oxidation to a biradical structure. The molecular design that involves the interruption of electronic delocalization between two units, one with electron donor character and therefore easily oxidizable, and another with electron acceptor character, a stable free radical, is a synthetic pathway to generate by oxidation processes biradical species with triplet

18

character. Our findings also show how small changes in the structure of these compounds can produce different kinds of oxidation processes which may be very helpful in designing new materials with different features.

Conflicts of interest

There are no conflicts to declare.

Acknowledgements

References

1. J. V. Grazulevicius, P. Strohriegl, J. Pielichowski and K. Pielichowski, *Prog. Polymer Sci.*, 2003, **28**, 1297-1353.
2. H. Higginbotham, K. Karon, P. Ledwon and P. Data, *Disp. Imaging*, 2017, **2**, 207-216.
3. G.-P. Chang, C.-N. Chuang, J.-Y. Lee, Y.-S. Chang, M.-k. Leung and K.-H. Hsieh, *Polymer*, 2013, **54**, 3548-3555.
4. K. Karon and M. Lapkowski, *J. Solid State Electrochem.*, 2015, **19**, 2601-2610.
5. S.-K. Chiu, Y.-C. Chung, G.-S. Liou and Y. O. Su, *J. Chin. Chem. Soc.*, 2012, **59**, 331-337.
6. S.-H. Hsiao, S.-C. Peng, Y.-R. Kung, C.-M. Leu and T.-M. Lee, *Eur. Polym. J.*, 2015, **73**, 50-64.
7. P. Ledwon, P. Zassowski, T. Jarosz, M. Lapkowski, P. Wagner, V. Cherpak and P. Stakhira, *J. Mat. Chem. C*, 2016, **4**, 2219-2227.
8. D. Gudeika, J. V. Grazulevicius, D. Volyniuk, R. Butkute, G. Juska, A. Miasojedovas, A. Gruodis and S. Jursenas, *Dyes Pigm.*, 2015, **114**, 239-252.
9. M. Reig, G. Bagdziunas, D. Volyniuk, J. V. Grazulevicius and D. Velasco, *Phys.Chem.Chem.Phys.*, 2017, **19**, 6721-6730.
10. O. Armet, J. Veciana, C. Rovira, J. Riera, J. Castaner, E. Molins, J. Rius, C. Miravitlles, S. Olivella and J. Brichfeus, *J. Phys. Chem. A*, 1987, **91**, 5608-5616.
11. A. Gilabert, L. Fajarí, I. Sirés, M. Reig, E. Brillas, D. Velasco, J. M. Anglada and L. Juliá, *New J. Chem.*, 2017, **41**, 8422-8430.
12. V. Gamero, D. Velasco, S. Latorre, F. Lopez-Calahorra, E. Brillas and L. Julia, *Tetrahedron Lett.*, 2006, **47**, 2305-2309.
13. D. Velasco, S. Castellanos, M. Lopez, F. Lopez-Calahorra, E. Brillas and L. Julia, *J. Org. Chem.*, 2007, **72**, 7523-7532.
14. S. Castellanos, D. Velasco, F. Lopez-Calahorra, E. Brillas and L. Julia, *J. Org. Chem.*, 2008, **73**, 3759-3767.
15. M. Lopez, D. Velasco, F. Lopez-Calahorra and L. Julia, *Tetrahedron Lett.*, 2008, **49**, 5196-5199.

16. S. Castellanos, V. Gaidelis, V. Jankauskas, J. V. Grazulevicius, E. Brillas, F. Lopez-Calahorra, L. Julia and D. Velasco, *Chem. Commun.*, 2010, **46**, 5130-5132.

17. L. Fajarí, R. Papoular, M. Reig, E. Brillas, J. L. Jorda, O. Vallcorba, J. Rius, D. Velasco and L. Juliá, *J. Org. Chem.*, 2014, **79**, 1771-1777.

18. M. Reig, C. Gozalvez, V. Jankauskas, V. Gaidelis, J. V. Grazulevicius, L. Fajari, L. Julia and D. Velasco, *Chem. Eur. J.*, 2016, **22**, 18551-18558.

19. Y. Gao, W. Xu, H. Ma, A. Obolda, W. Yan, S. Dong, M. Zhang and F. Li, *Chem. Mater.*, 2017, **29**, 6733-6739.

20. S. Dong, A. Obolda, Q. Peng, Y. Zhang, S. Marder and F. Li, *Mater. Chem. Front.*, 2017, **1**, 2132-2135.

21. X. Ai, E. W. Evans, S. Dong, A. J. Gillett, H. Guo, Y. Chen, T. J. H. Hele, R. H. Friend and F. Li, *Nature*, 2018, **563**, 536-540.

22. A. D. Becke, *J. Chem. Phys.*, 1993, **98**, 5648-5652.

23. F. Trani, G. Scalmani, G. Zheng, I. Carnimeo, M. J. Frisch and V. Barone, *J. Chem. Theor. Comput.*, 2011, **7**, 3304-3313.

24. Y. Guo, C. Riplinger, U. Becker, D. G. Liakos, Y. Minenkov, L. Cavallo and F. Neese, *J. Chem. Phys.*, 2018, **148**, 011101.

25. J. F. Ambrose, L. L. Carpenter and R. F. Nelson, *J. Electrochem. Soc.* , 1975, **122**, 876-894

26. L. He, G. Bester and A. Zunger, *Phys. Rev. B*, 2005, **72**, 195307.

27. W. B. Gleason and R. E. Barnett, *J. Am. Chem. Soc.*, 1976, **98**, 2701-2705.

Physical Chemistry Chemical Physics Accepted Manuscript

Table of Contents
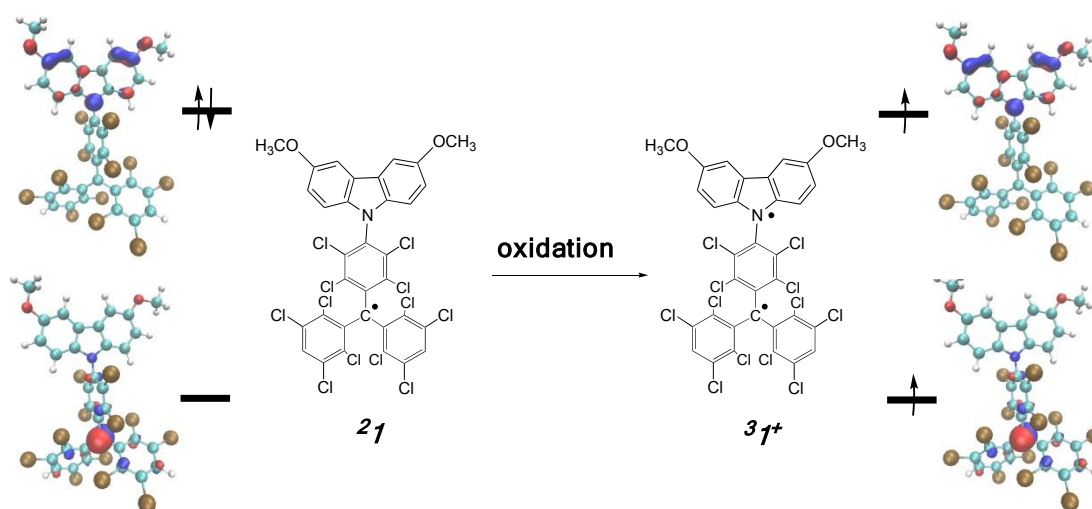
The oxidation of the dimethoxicarbazole adduct of tris(2,3,5,6-tetrachlorophenyl)methyl radical (DTM) involves one electron from the HOMO orbital rather than from the SOMO, to generate a triplet state.